Journal of Alzheimer's Disease 44 (2015) 949–962
DOI 10.3233/JAD-142076
IOS Press

Bone Marrow-Derived Macrophages from AβPP/PS1 Mice are Sensitized to the Effects of Inflammatory Stimuli

James P. Barrett, Aedín M. Minogue, Raasay S. Jones, Catia Ribeiro, Ronan J. Kelly and Marina A. Lynch*
Trinity College Institute of Neuroscience, Trinity College, Dublin 2, Ireland

Accepted 3 October 2014

Abstract. Macrophages are key cells in tissue defense in the periphery and, under certain circumstances, infiltrate the central nervous system, where they may play a similar role in the brain, perhaps supporting the function of microglia. Macrophages have been shown to adopt different activation states in response to various stimuli. Specifically, when exposed to inflammatory stimuli such as interferon (IFN)γ, the cells adopt the M1 phenotype, whereas when exposed to anti-inflammatory cytokines such as interleukin (IL)-4 or IL-13, the M2 phenotype is adopted. While M1 macrophages are associated with tissue defense and destruction of invading pathogens, M2 macrophages are involved in tissue repair and in terminating inflammation. It is well known that an inflammatory microenvironment exists in the brain of aged animals and also in the brain of mice that overexpress amyloid-β protein precursor (AβPP) and presenilin 1 (PS1; AβPP/PS1 mice), a commonly-used model of Alzheimer's disease (AD). Recent studies have revealed that immune cells, including macrophages, infiltrate the brain in both circumstances raising the possibility that these cells adopt the M1 activation state and contribute to the already-existing neuroinflammation. We set out to examine the responses of bone marrow-derived macrophages prepared from wildtype and AβPP/PS1 mice and demonstrate that cells from AβPP/PS1 mice, even after several days in culture, respond more profoundly to IFNγ than those from wildtype mice. We suggest that this propensity to respond to M1-polarizing stimuli, together with the described changes in the brain of AβPP/PS1 mice, contribute to the development of chronic neuroinflammation.

Keywords: AβPP/PS1 mice, blood-brain barrier, bone marrow-derived macrophages, IFNγ, M1 and M2 phenotypes, neuroinflammation

INTRODUCTION

Macrophages are particularly plastic cells adopting different phenotypes in response to various stimuli. They are broadly divided into the M1 proinflammatory phenotype, induced by stimuli interferon (IFN)γ and lipopolysaccharide (LPS), and the M2 anti-inflammatory phenotype induced by anti-inflammatory cytokines such as interleukin (IL)-4 and IL-13 [1, 2]. M1 macrophages are involved in tissue defense and are characterized by increased expression of inflammatory markers such as tumor necrosis factor (TNF)α and nitric oxide synthase (NOS)2, whereas M2 macrophages are responsible for terminating the inflammatory response, initiating tissue repair and re-establishing homeostasis; consequently these cells are identified by markers including arginase 1 (Arg1) and mannose receptor (MRC1).

Microglia are considered to be the macrophage equivalent in the brain and, as such, share many of their properties [3]; the evidence indicates that microglia react to polarizing stimuli in a manner that resembles the response of macrophages adopting similar M1 and M2 activation states [4, 5]. Microglia, like macrophages, are professional phagocytes, although it has been suggested that their phagocytic capability is less than that of macrophages [6]. Previous reports have

*Correspondence to: Prof. Marina A. Lynch, Trinity College Institute of Neuroscience, Trinity College, Dublin 2, Ireland. Tel.: +353 1 8968531; Fax: +353 1 8963545; E-mail: lynchma@tcd.ie.

ISSN 1387-2877/15/$35.00

suggested that decreased recruitment of mononuclear cells into the central nervous system (CNS) coincides with an increased plaque burden in an animal model of Alzheimer's disease (AD) [7]. Indeed the phagocytic efficiency of macrophages, in addition to their ability to participate in tissue repair, has led to the proposal that these cells may play an important role in neuroprotection [8] particularly in situations of acute insult [9]. For example, it has been reported that macrophages, which are found in the spinal cord following traumatic injury, participate in tissue recovery [10], though the likelihood that they adopt the M1, rather than the M2, phenotype when they encounter the inflammatory microenvironment has been raised [11].

The amyloid-β protein precursor (AβPP)/presenilin 1 (AβPP/PS1) model is one of the most commonly-used mouse models of AD. The presence of amyloid-β (Aβ) plaques in the brains of AβPP/PS1 mice has been observed as early as 4 months of age and plaque numbers increase with age [12]. These mice exhibit memory deficits [13, 14], as well as evidence of enhanced microglial activation [15]. Recent evidence has indicated that blood-brain barrier (BBB) permeability is increased with age and in AβPP/PS1 mice [16, 17], and this is accompanied by the presence of IFNγ-producing peripheral immune cells in the brain [17]. Data from this laboratory has demonstrated that the pathology seems to progress with age [22]. An increase in the number of infiltrating macrophages, and evidence of enhanced expression of the inflammatory cytokines IL-1β, TNFα, and IFNγ has also been observed in the brain with age and in AβPP/PS1 mice [15, 18, 19]. Therefore, when macrophages infiltrate the brain in these models, they encounter a proinflammatory microenvironment which may stimulate the cells to adopt the M1 phenotype. Here, we set out to compare the responses of macrophages prepared from the bone marrow of AβPP/PS1 mice and wildtype (WT) mice to polarizing stimuli. The data indicate that bone marrow-derived macrophages (BMDMs) from AβPP/PS1 mice are more responsive to LPS and IFNγ whereas their response to IL-4 is not genotype-specific.

MATERIALS AND METHODS

Animals

Groups of male and female 15–24 month-old AβPPswe/PS1dE9 mice, hereafter referred to as AβPP/PS1 mice, expressing a chimeric mouse/human amyloid precursor protein (Mo/HuAPP695Swe) and a mutant human presenilin 1 (PS1-dE9), were used in this study. AβPP/PS1 (Jackson Laboratories, Maine, USA) and WT littermate mice were bred in an SPF animal housing facility in the Bioresources Unit, Trinity College Dublin and maintained under veterinary supervision in a controlled environment (12-h light-dark cycle; 22–23°C). All experimental work was performed under a license granted by the Minister for Health and Children (Ireland) under the Cruelty to Animals Act 1876 and the European Community Directive 86/609/EEC. Groups of WT and AβPP/PS1 mice were comprised of similar numbers of males and females and an even spread of ages. No differences in responses of BMDMs prepared from male or female mice were observed. Whole blood was collected from WT and AβPP/PS1 mice by transcardial perfusion, diluted 1 : 1 with sterile 1X phosphate-buffered saline (PBS), overlaid on Lymphoprep^{TM} (2 ml; Axis-Shield, UK) and centrifuged with the brake off ($600 \times g$, 30 min). Serum was collected to the level of the interface and stored at −80°C for treatment of endothelial cells. Mice were killed by decapitation, and the brain was rapidly removed and placed on ice. The hippocampi were dissected free from each hemisphere, flash-frozen, and stored at −80°C for later analysis.

Preparation, culture, and treatments of BMDMs

BMDMs were isolated from the marrow of the femurs and tibias of WT and AβPP/PS1 mice. The legs of the animals were sprayed with 70% EtOH and the skin and muscle tissue removed from the bones. The bones were sprayed with 70% EtOH, transferred to a sterile flow hood and cut at both ends. The marrow was flushed out into a sterile falcon tube in Dulbecco's modified Eagle's medium (DMEM; 500 ml; Invitrogen, UK) supplemented with heat-inactivated fetal bovine serum (FBS; 50 ml; 10%; Gibco, UK) and penicillin-streptomycin (5 ml; 1%; Gibco, UK). The cell suspension was triturated using a sterile Pasteur pipette, filtered through a nylon mesh filter (40 μm; BD Biosciences, US) into a sterile tube and centrifuged ($400 \times g$, 5 min). The supernatant was removed and the pellet resuspended in red blood cell lysis buffer (Sigma Aldrich, UK). The suspension was centrifuged ($400 \times g$, 5 min), the supernatant discarded, cells washed using DMEM and centrifuged once more ($400 \times g$, 5 min). The pellet was resuspended in DMEM supplemented with L929 conditioned media (20%). Cells were seeded in sterile cell culture T75 cm^2 flasks. On day 2, non-adherent cells were removed from the flask and media replaced, these cells remained in culture for a further 6 days, with

media being replaced on day 4. On day 6, cells were transferred to 6-well plates (0.5×10^6 cells per well) and remained in culture for a further 2 days. Cells were incubated in the presence of LPS (100 ng/ml; from Escherichia coli; Enzo Life Sciences, UK), IFNγ (50 ng/ml; R&D Systems, UK), or IL-4 (200 ng/ml; R&D Systems, UK) for 24 h, supernatants were collected for analysis of cytokines by ELISA and cells were harvested for analysis of markers of macrophage activation by real-time PCR and flow cytometry; the concentrations of LPS, IFNγ, and IL-4 were selected based on the findings of previous studies [20, 21]. The purity of the BMDM culture was assessed by flow cytometric analysis. BMDMs were identified as $CD11b^+CD45^{high}$ cells, and it was found that >98% of the cells in culture were positive for both of these markers. Furthermore, >95% of these $CD11b^+CD45^{high}$ cells were also positive for CD68.

Analysis of blood-brain barrier permeability by magnetic resonance imaging (MRI)

To assess BBB permeability, we evaluated the signal derived from extravasation of the gadolinium-based contrast agent gadopentate dimeglumine (Clissmann, Ireland). Mice were anaesthetized with 4% isoflurane (Isoflo, Abbott Animal Health, UK) in 100% oxygen by placing them in a clear plastic chamber connected to an anesthetic scavenging system, and filling the chamber with the gas mixture; anesthesia was maintained by delivery of a mixture of isoflurane and oxygen (1.5–2% at 1 liter/min of 100% oxygen). Mice were placed in a specially-designed cradle in a small rodent Bruker Biospec system with a 7 Tesla magnet and a 30 cm core (Bruker Biospin, Germany) and the right lateral tail vein was cannulated to permit delivery of gadopentate dimeglumine. Thus, pre- and post-contrast measurements were determined within the same contrast scan without moving the animal. Contrast imaging was carried out using a T1-weighted fast low angle shot (FLASH) sequence (10 repetitions; 1 repetition time: 2 min, 11 s; dimensions = 128×128 voxels per slice). Baseline measurements were acquired on repetition 1, prior to injection of the contrast agent, which was injected at the start of repetition 2. Gadolinium-enhanced contrast images were analyzed using Medical Image Processing, Analysis, and Visualization (MIPAV) software. Anatomically-distinct regions of interest viewed in repetition 1 were overlayed with a 2×2 voxel square, and the average pre-contrast intensity measured. Values for each data set were normalized to the pre-contrast measurement and expressed relative to the pre-contrast value.

Cell culture

Mouse brain-derived endothelial cells (bEnd3; ATCC, UK) were grown to confluence in T25 cm^2 flasks in DMEM (ATCC, UK) containing 10% FBS and 1% penicillin-streptomycin (Invitrogen, UK). When confluence was achieved, cells were transferred to 6-well plates (0.5×10^6 well) and maintained in culture for a further 24 h. Cells were incubated with DMEM containing serum (5%) from WT or AβPP/PS1 mice for 3 h after which time cells were harvested and fractionation carried out using a Subcellular Protein Fractionation kit for Cultured Cells as per manufacturer's instructions (Pierce, UK).

PAGE and western blotting

Cytosolic and membrane fractions were assessed for protein expression by electrophoresis and western immunoblotting as previously described [22]. Primary antibodies against claudin-5 (1 : 2000; Invitrogen, UK), occludin (1 : 1000; BD Transduction, UK), zona occludens (ZO)-1 (1 : 1000; Invitrogen, UK) and phosphorylated c-Jun terminal kinase (JNK; 1 : 1000; Cell Signaling Technology, USA) were used with horseradish peroxidase-conjugated secondary antibodies (1 : 10,000; Jackson ImmunoResearch, UK). Bands were visualized using Supersignal West Pico Chemiluminescent Substrate (Thermo Scientific, USA) and images were captured using a Fujifilm LAS-3000 (Brennan & Co., Ireland).

Analysis of mRNA expression by real-time PCR

RNA was isolated from BMDMs or from hippocampal tissue using a Nucleospin® RNAII kit (Macherey-Nagel GmbH, Germany) and reverse transcribed into cDNA using a High-Capacity cDNA Archive kit (Applied Biosystems, UK) as per manufacturer's instructions. Assay IDs for the genes examined were as follows: β-actin (4352341E), TNFα (Mm00443258_m1), NOS2 (Mm0040502_m1), Nucleotide-binding oligomerization domain-containing protein 2 (NOD2) (Mm00467543_m1), CD40 (Mm00441891_m1), CD86 (Mm01344638_m1), MRC1 (Mm00485148_m1), Arg1 (Mm00475988_m1), interferon γ-induced protein 10 (IP-10) (Mm00445235_m1), monocyte chemoattractant protein-1 (MCP-1) (Mm00441242_m1), IFNγR1

(Mm00599890_m1), and IL-4Rα (Mm01275139_m1). Real-time PCR was performed using an ABI Prism 7300 instrument (Applied Biosystems, UK) with β-actin used as the endogenous control. No age-related change in β-actin was observed. In all cases, relative gene expression was calculated with reference to untreated BMDMs from WT mice using the ΔΔCT method with Applied Biosystems RQ software (Applied Biosystems, UK).

Analysis of inflammatory cytokines by ELISA

IFNγ concentration was measured in hippocampal homogenates (4 mg/ml protein concentration) by ELISA (R&D Systems, DY485) as previously described [22] and TNFα and IL-1β concentrations were assessed in supernatant samples obtained from BMDMs. Standard curves were prepared using recombinant proteins diluted in the appropriate buffers as recommended by the manufacturers (PBS containing 1% BSA for brain tissue and DMEM for supernatant samples). Briefly, standards or samples (100 μl) were added to antibody-coated 96-well plates and incubated for 2 h at room temperature, plates were washed and samples were incubated in detection antibody for 2 h. Plates were washed and incubated in horseradish peroxidase-conjugated streptavidin (1 : 200 in PBS containing 1% BSA) for 20 min at room temperature. Substrate solution (tetramethylbenzidine; Sigma, UK) was added, incubation continued at room temperature in the dark for 30 min and the reaction was stopped using H_2SO_4 (1 M). Absorbance measurements were read at 450 nm using a microplate reader (Bio Tek Instruments, USA). Protein concentrations were calculated relative to the appropriate standard curve and expressed as pg/mg brain tissue and the lower limits of detection for IFNγ, TNFα, and IL-1β were 31.2, 31.2, and 15.6 pg/ml, respectively. Cytokine concentrations for all samples measured lay within the appropriate detection range, however, in the case of IFNγ, measured values were adjusted to reflect pg of IFNγ per mg protein.

Flow cytometry

To assess the presence of macrophages in the brain, mice were transcardially perfused with ice-cold PBS, brain tissue was dissected free and the meninges removed. The cerebellum was removed and discarded, the corpus callosum and white matter were also removed, and the hippocampus was dissected free and stored for later analysis. The remaining tissue was placed in 1X Hank's Balanced Salt Solution (HBSS; Invitrogen, UK), cross-chopped, homogenized and triturated using fire-polished Pasteur pipettes with three decreasing diameters. Cell suspensions were filtered through a cell strainer (70 μM) and cells pelleted by centrifugation (200 × g, 10 min). Cells were resuspended in 70% Percoll (9 ml), underlaid with 100% Percoll (5 ml), and overlaid with 57% Percoll (9 ml), 21.5% Percoll (9 ml), and 1X PBS (9 ml). The gradients were centrifuged (1250 × *g*, 45 min), mononuclear cells were collected from the 57–70% and 21.5–57% interfaces, and flow cytometric analysis was undertaken as previously described [22]. Cells were blocked in FACS buffer containing purified anti-mouse CD16/CD32 (1 : 100; BD Biosciences, UK) and infiltrating macrophages were identified by staining for PE-Cy7 anti-mouse CD45 (1 : 100, Bioscience, UK) and Alexa Fluor 647 anti-mouse CD11b (1 : 100; BD Biosciences, UK). A forward versus side scatter gating strategy was employed to exclude debris and dead cells which have characteristically low forward and high side scatter signals. Macrophages are presented as the number of $CD11b^{+}CD45^{high}$ cells within this live cell population, a strategy commonly employed to identify these cells [23–26]. BMDMs in culture were also identified as $CD11b^{+}CD45^{high}$ cells and examined for expression of PE anti-mouse CD40 (1 : 100; BD Biosciences, UK) and Alexa Fluor 488 anti-mouse MRC1 (1 : 100, BioLegend, UK) following treatment. To assess phagocytosis, BMDMs were incubated with amyloid-β (1-42) HiLyte™ Fluor 488-labeled (0.5 μM; Anaspec, USA) for 2 h following treatment with IFNγ or IL-4, as described above. Media was replaced with trypan blue (0.2 mg/ml; Sigma, UK) and samples were incubated for 2 min to quench extracellular fluorescence. Phagocytic cells were represented as the number of $CD11b^{+}CD45^{high}$ cells positive in the fluorescein isothiocyanate (FITC) channel. Immunofluorescence was read immediately on a DAKO CyAn-ADP 7 color flow cytometer with Summit software v4.3 for acquisition. BD™ CompBeads (BD Bioscience, UK) were used to optimize fluorescence settings and further flow cytometric analysis was carried out in FlowJo v7.6.5. Unstained cells and fluorescence minus one (FMO) tubes were used to gate the percentage of positive cells in any channel.

Statistical analysis

All data are expressed as mean ± standard error of the mean (SEM). Data were analyzed using a Student's *t*-test for independent means or 2-way analysis

of variance (ANOVA) where indicated followed by a Bonferroni *post hoc* test. MRI data were analyzed using a repeated measures ANOVA with genotype and repetition as variables. In addition, a Student's *t*-test was carried out on the data obtained at the last repetition. Analysis was carried out using Prism software (Graphpad, US).

RESULTS

Infiltration of macrophages into the brain of AβPP/PS1 mice is associated with BBB permeability

The findings indicate that there is an increase in macrophage infiltration into the brain of AβPP/PS1 mice ($^{**}p < 0.01$; Student's *t*-test; Fig. 1A). Infiltrating macrophages were identified as $CD11b^{+}CD45^{high}$ cells, which are distinct from $CD11b^{+}CD45^{low}$ microglia (Fig. 1B). The increase in macrophages is associated with an increase in expression of IFNγR on BMDMs prepared from AβPP/PS1 mice ($^{*}p < 0.05$; Student's *t*-test; Fig. 1C) and a genotype-related increase in IFNγ concentration in brain tissue ($^{*}p < 0.05$; Student's *t*-test; Fig. 1D). Peripheral cells are generally excluded from the brain but can infiltrate as a consequence of a chemotactic signal or an increase in BBB permeability. Thus, significant genotype- and time (repetition)-related increases in signal intensity derived from extravasated gadolinium were observed in the motor cortex ($p < 0.01$ and $p < 0.001$ for genotype and time respectively; 2-way ANOVA; Fig. 1E) and entorhinal cortex ($p < 0.001$ for both genotype and time; Fig. 1E). Analysis of the mean value obtained at the last repetition revealed a genotype-related increase in BBB permeability ($p < 0.01$; Fig. 1E, F; Student's *t*-test). These data support previous findings which indicated that BBB permeability in several areas of the brain, including hippocampus, was associated with infiltrating cells in the brain of AβPP/PS1 mice [22]. Furthermore, we report a genotype-related increase in hippocampal mRNA expression of two chemokines, MCP-1 and IP-10 ($^{*}p < 0.05$; Student's *t*-test; Fig. 1G, H), both of which are chemoattractant for macrophages [3].

Serum from AβPP/PS1 mice alters tight junction (TJ) protein expression in an endothelial cell line

An intact BBB provides an important protective strategy for limiting the entry of cells into the brain. Given the enhanced BBB permeability in AβPP/PS1 mice, the impact of circulating factors on BBB integrity was assessed by incubation of an endothelial cell line with serum obtained from WT or AβPP/PS1 mice. The membrane expression of claudin-5 and occludin, two proteins integral to BBB function, were significantly decreased in endothelial cells exposed to serum from AβPP/PS1, compared with WT, mice ($^{**}p < 0.01$; $^{***}p < 0.001$; Student's *t*-test; Fig. 2A, B respectively). The cytosolic expression of ZO-1, a protein involved in stabilization of the TJ, was significantly decreased in endothelial cells exposed to serum from AβPP/PS1, compared with WT, mice ($^{**}p < 0.01$; Student's *t*-test; Fig. 2C). Interestingly, the expression of the phosphorylated form of the stress-activated protein kinase JNK was significantly enhanced in endothelial cells exposed to serum from AβPP/PS1, compared with WT, mice ($^{*}p < 0.05$; Student's *t*-test; Fig. 2D). Several studies have linked cytokine secretion, including IL-1β, to BBB disruption [27] and a number of pro-inflammatory cytokines were increased in serum from AβPP/PS1 mice (Table 1).

BMDMs from AβPP/PS1 mice are more responsive to IFNγ than those from WT mice

As macrophages enter the brain in AβPP/PS1 mice and encounter an inflammatory environment [15, 17, 28], including increased IFNγ concentration as described above, the possibility exists that the infiltrating cells will adopt the M1 inflammatory phenotype. We assessed the responsiveness of BMDMs, prepared from WT and AβPP/PS1 mice, to polarizing stimuli IFNγ and IL-4. IFNγ significantly increased the mRNA expression of some markers of the M1 activation state [3, 29, 30] including TNFα and NOS2 in cells from WT mice ($^{***}p < 0.001$; ANOVA; Fig. 2A, C) and this IFNγ-induced effect was enhanced in cells from AβPP/PS1 mice ($^{+}p < 0.05$; $^{++}p < 0.01$; ANOVA; Fig. 3A, C). Whereas IFNγ exerted no significant effect on supernatant concentrations of TNFα and IL-1β in cells from WT mice, it increased release of both proteins from AβPP/PS1 BMDMs ($^{*}p < 0.05$; ANOVA; Fig. 3B, D). While IFNγ increased CD40 mRNA and protein expression on BMDMs ($^{***}p < 0.001$; ANOVA; Figs. 4A, B),

Table 1
Serum cytokines are increased in AβPP/PS1 mice

	WT	AβPP/PS1
IL-6	5.3 (3.4)	161.5 (67.4)
IL-12	ND	98.9 (64)
CXCL1	135.7 (24.7)	275.8 (81.9)
IFNγ	0.31 (0.31)	6.7 (1.8)

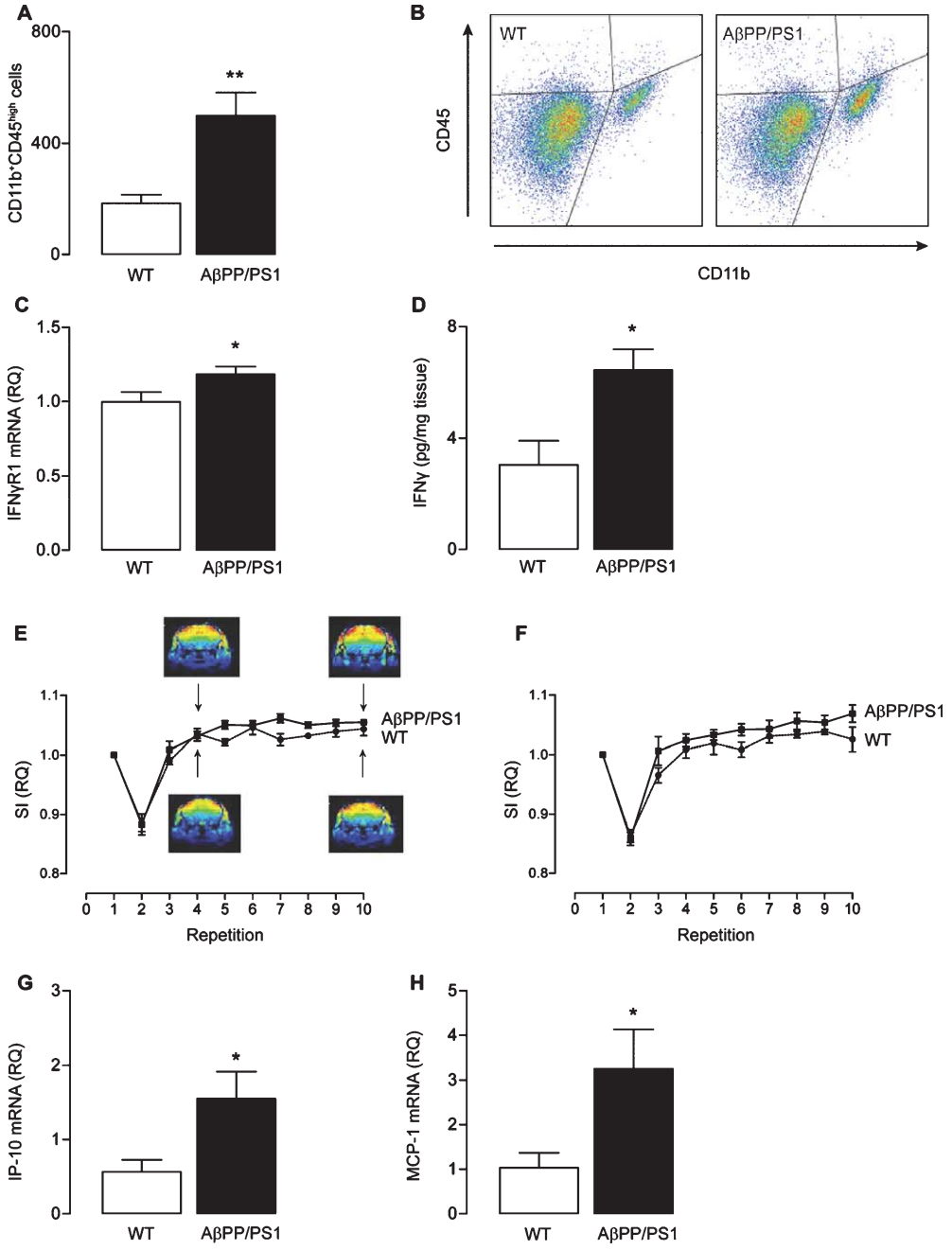

Fig. 1. Enhanced BBB permeability in AβPP/PS1 mice is associated with an increase in macrophage infiltration and chemokine expression. The number of $CD11b^{+}CD45^{high}$ macrophages was increased in the brain of AβPP/PS1, compared with WT, mice (A; $^{**}p<0.01$; Student's *t*-test; $n=10$–12). Macrophages were identified as $CD11b^{+}CD45^{high}$ cells, which are distinct from $CD11b^{+}CD45^{low}$ microglia; representative FACS plots are shown (B). IFNγR1 mRNA expression was increased in BMDMs prepared from AβPP/PS1, compared with WT, mice (C; $^{*}p<0.05$; Student's *t*-test; $n=10$–12). IFNγ concentration was significantly greater in the hippocampus of AβPP/PS1, compared with WT, mice (D; $^{*}p<0.05$; Student's *t*-test; $n=8$–10). Gadolinium-enhanced contrast imaging was used to assess BBB permeability in WT and AβPP/PS1 mice. Gadolinium was injected at the commencement of repetition 2. At the end of repetition 10, mean signal intensity (SI) was significantly greater in the motor (E) and entorhinal (F) cortices of AβPP/PS1 compared with WT mice ($^{**}p<0.01$; Student's *t*-test; $n=4$–6). Analysis of the data by 2-way ANOVA revealed significant genotype ($p<0.01$ and $p<0.001$) and repetition ($p<0.001$) effects in motor and entorhinal cortices respectively. Values are presented as a proportion of the pre-contrast measure (repetition 1) and are means ± SEM. Representative color enhanced images for repetitions 4 and 10 are presented for WT and AβPP/PS1 mice. Hippocampal expression of MCP-1 (G) and IP-10 (H) mRNA was significantly greater in AβPP/PS1, compared with WT, mice ($^{*}p<0.05$; Student's *t*-test; $n=8$–10). Values are means ± SEM.

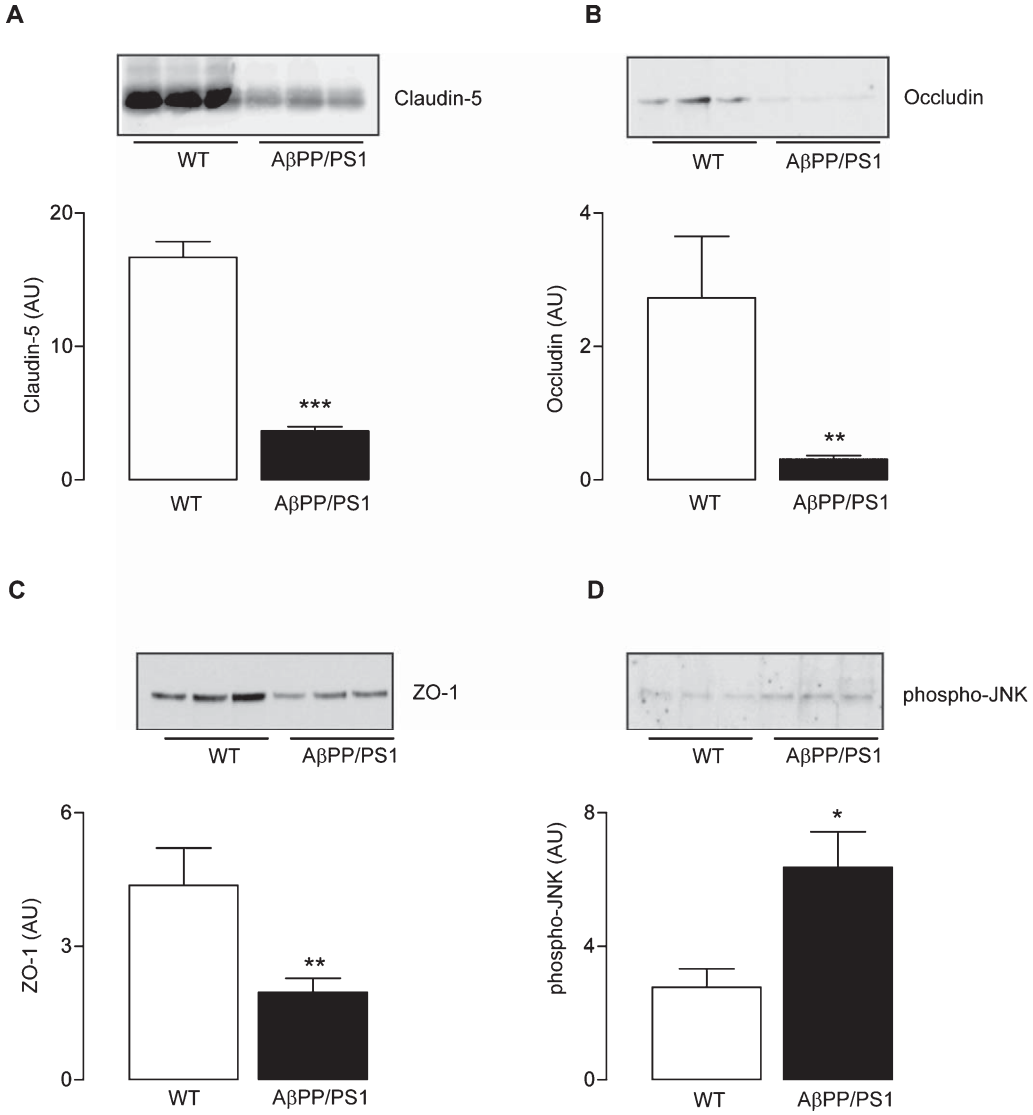

Fig. 2. Serum from AβPP/PS1 mice negatively impacts on TJ integrity in endothelial cells. Endothelial cells were incubated with serum from WT or AβPP/PS1 mice (3 h). Membrane expression of the TJ proteins claudin-5 (A) and occludin (B) were significantly decreased in endothelial cells incubated with serum from AβPP/PS1, compared with WT, mice ($^{**}p < 0.01$; $^{***}p < 0.001$; Student's *t*-test; $n = 3$). Cytosolic expression of ZO-1 was decreased in endothelial cells incubated with serum from AβPP/PS1, compared with WT, mice ($^{**}p < 0.01$; Student's *t*-test; $n = 3$). Expression of phosphorylated JNK was enhanced in endothelial cells stimulated with serum from AβPP/PS1, compared with WT, mice ($^{*}p < 0.05$; Student's *t*-test; $n = 3$). Representative immunoblots are shown and values are means ± SEM.

no genotype-related effect of IFNγ was observed in either case. NOD2 and CD86 expression are also considered to be markers of the M1 phenotype [3, 29, 30], and we found that expression of both were increased in cells from WT and AβPP/PS1 mice following IFNγ stimulation ($^{***}p < 0.001$; ANOVA; Figs. 4C, D). This effect was significantly enhanced in cells from AβPP/PS1 mice ($^{++}p < 0.01$; ANOVA; Figs. 4C, D). These data suggest that when infiltrating macrophages are exposed to the inflammatory environment that characterizes the brain of AβPP/PS1 mice, they respond by adopting the M1 phenotype; this response includes an increase in release of TNFα and IL-1β which potentially exacerbates the pre-existing inflammation.

BMDMs from AβPP/PS1 mice are more responsive to LPS than BMDMs from WT mice

Incubation of cells in the presence of LPS also induced a significant increase in mRNA expression of TNFα and NOS2 ($^{***}p < 0.001$; ANOVA; Table 2) and

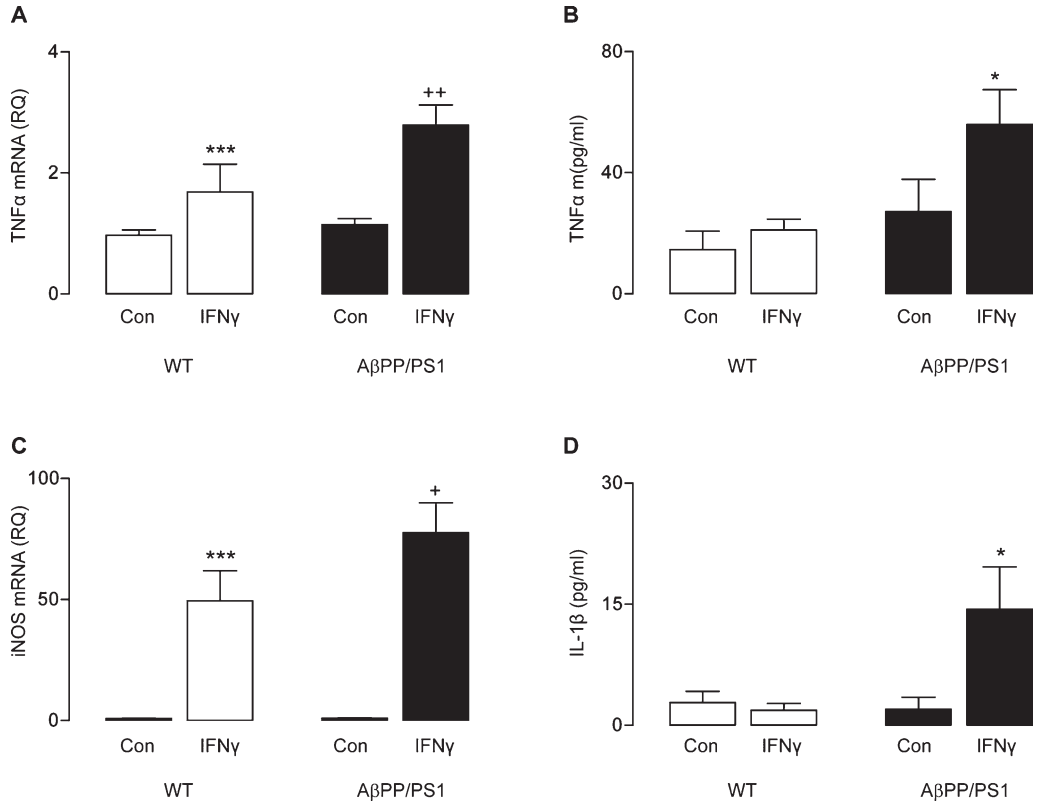

Fig. 3. IFNγ increased mRNA expression of TNFα, NOS2 and IL-1β in BMDMs from WT and AβPP/PS1 mice. IFNγ significantly increased TNFα (A) and NOS2 (C) mRNA expression in BMDMs from WT and AβPP/PS1 mice ($^{***}p < 0.001$; ANOVA; $n = 10$–12). The IFNγ-induced effect on TNFα and NOS2 mRNA was significantly greater in BMDMs prepared from AβPP/PS1 mice ($^{+}p < 0.05$; $^{++}p < 0.01$; ANOVA). Release of TNFα (B) and IL-1β (D) were significantly enhanced in IFNγ-stimulated BMDMs prepared from AβPP/PS1, compared with wildtype, mice ($^{*}p < 0.05$; ANOVA; $n = 3$). Values are means ± SEM.

the LPS-induced effect on TNFα and NOS2 mRNA was significantly enhanced in cells from AβPP/PS1 mice ($^{+}p < 0.05$; ANOVA; Table 2). Mean expression of TLR4 mRNA was significantly greater in BMDMs prepared from AβPP/PS1 mice (1.43 ± 0.07, SEM) compared with WT mice (1.02 ± 0.07; *** $p < 0.001$; Student's *t*-test for independent means; Table 2).

IL-4 exerts a similar effect on BMDMs from AβPP/PS1 and WT mice

Incubation of BMDMs with IL-4 significantly increased mRNA expression of Arg1 and MRC1, archetypal markers of the M2 phenotype ($^{***}p < 0.001$; ANOVA; Figs. 5A, B), however the effect of IL-4 was similar on cells from WT and AβPP/PS1 mice. IL-4 also increased the expression of MRC1 on BMDMs and the effect was similar in cells from WT and AβPP/PS1 mice ($^{***}p < 0.01$; ANOVA; Fig. 5C). No genotype-related change was observed in IL-4Rα mRNA expression on BMDMs from WT and AβPP/PS1 mice (Fig. 5D).

IFNγ decreases, while IL-4 increases, the ability of BMDMs to phagocytose Aβ

To identify a functional phenotype associated with M1 and M2 BMDMs, we compared the ability of

Table 2
LPS increased mRNA expression of TNFα and NOS2 in macrophages from WT and AβPP/PS1 mice

	WT		AβPP/PS1	
	Control	LPS	Control	LPS
TNFα RNA	1.03 (0.06)	4.16 (0.56)***	1.02 (0.07)	5.91 (1.03)$^{+}$
NOS2 RNA	1.64 (0.48)	376.54 (123.60)***	3.14 (1.14)	1122.47 (509.48)$^{+}$
TLR4 RNA	1.02 (0.07)		1.43 (0.07)*	

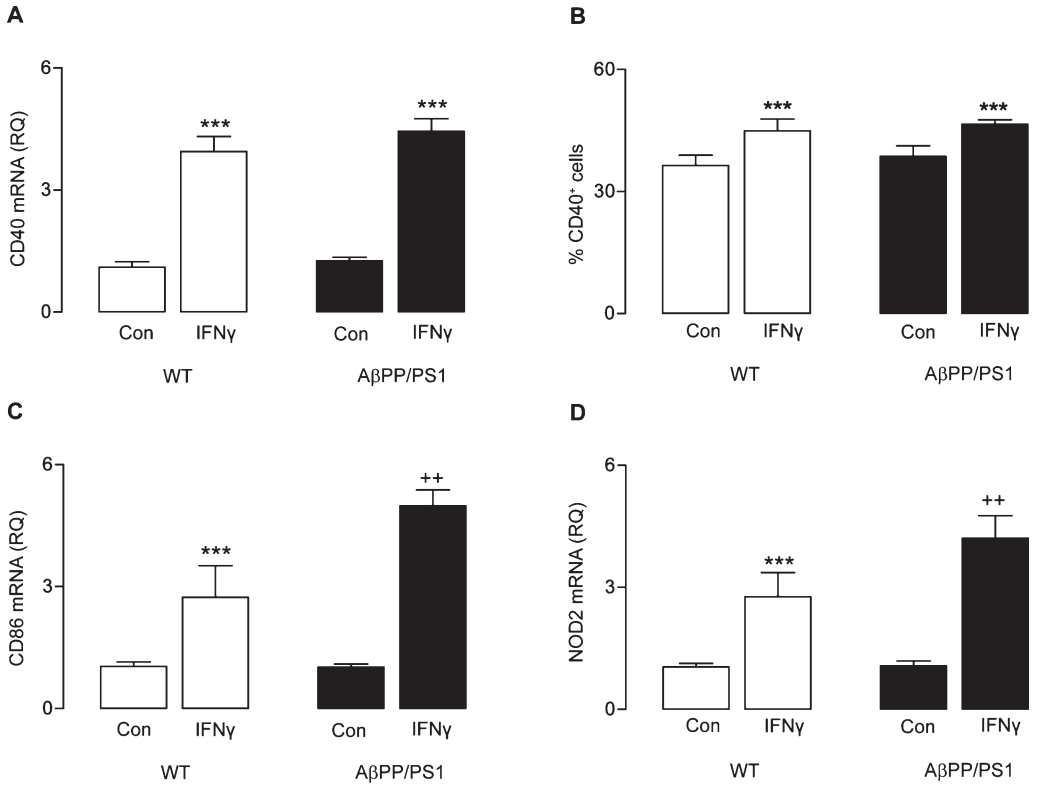

Fig. 4. IFNγ increased mRNA expression of CD40, CD86 and NOD2 in BMDMs from WT and AβPP/PS1 mice. IFNγ significantly increased CD40 (A), CD86 (C), and NOD2 (D) mRNA expression in BMDMs from WT and AβPP/PS1 mice (***$p < 0.001$; ANOVA; $n = 10$–12). The IFNγ-induced effect on CD86 and NOD2 mRNA was significantly enhanced in BMDMs prepared from AβPP/PS1 mice ($^{+}p < 0.05$; $^{++}p < 0.01$; ANOVA). IFNγ induced a significant increase in the expression of CD40 on BMDMs from WT and AβPP/PS1 mice, however no genotype-related increase was observed (***$p < 0.001$; ANOVA; $n = 3$). Values are means ± SEM.

IFNγ- and IL-4-treated cells from WT and AβPP/PS1 mice to phagocytose fluorescently-labelled Aβ. The data indicate that IFNγ-treated cells prepared from WT mice were less phagocytic than untreated controls (***$p < 0.001$; ANOVA; Fig. 6); an effect that was more profound in cells prepared from AβPP/PS1 mice ($^{+}p < 0.05$; ANOVA; Fig. 6). Conversely, phagocytosis of fluorescently-labelled Aβ was increased in IL-4-treated cells (***$p < 0.001$; ANOVA; Fig. 6) albeit to a lesser extent in cells prepared from AβPP/PS1 mice ($^{+}p < 0.05$; ANOVA; Fig. 6).

DISCUSSION

The significant finding in this study was that BMDMs prepared from AβPP/PS1 mice respond more profoundly to IFNγ than BMDMs from WT mice and that this was associated with increased mRNA expression of IFNγR. In contrast, there was no change in the responsiveness of BMDMs to IL-4, and also no change in mRNA expression of IL-4Rα. The importance of this finding lies in the fact that macrophages infiltrate the brain and encounter an environment in which IFNγ concentration is elevated; this has the potential to stimulate them to adopt the M1 phenotype and enhance the pre-existing neuroinflammation.

It appears that, in young AβPP/PS1 mice, $Ly6C^{low}CX3CR1^{high}CCR2^{-}$ monocytes are attracted to, and eliminate, the punctate Aβ accumulation around blood vessels suggesting that the cells may not need to infiltrate the parenchyma [31]. However, there is significant literature indicating that macrophages infiltrate the brain of mouse models of AD in both GFP-bone marrow chimeras [6, 32] and in mice which were not subjected to irradiation [33, 34]. The evidence suggests that macrophages are more efficient phagocytes than resident microglia [6] and, consistently, bone marrow transplantation was associated with decreased Aβ accumulation [35].

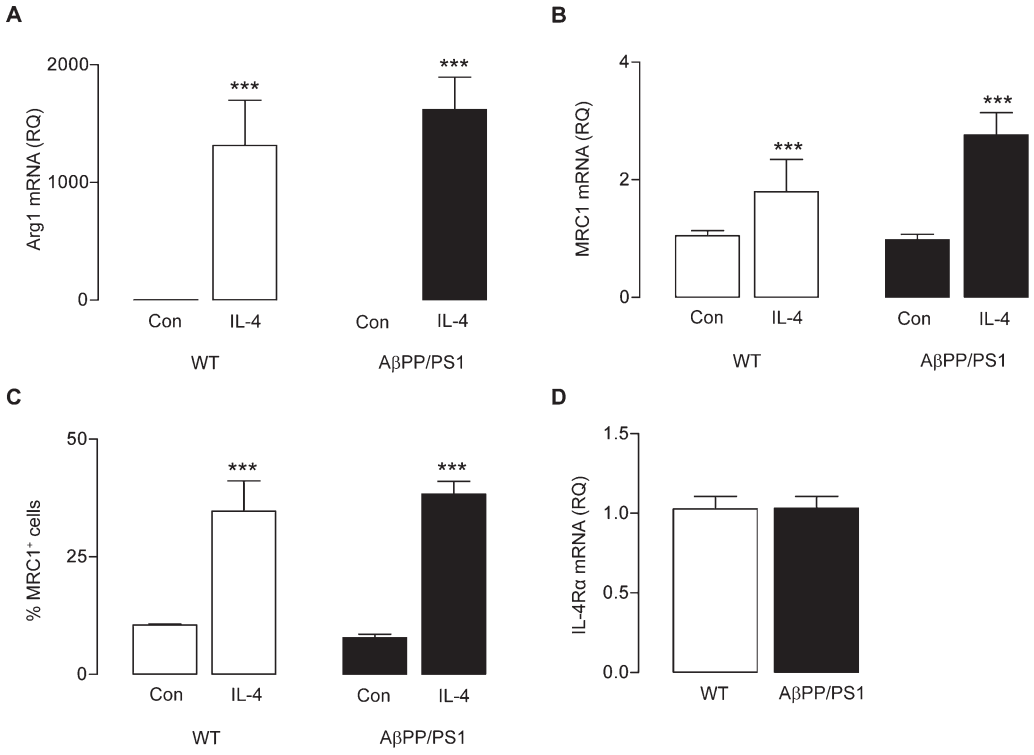

Fig. 5. IL-4 increased mRNA expression of Arg1 and MRC1 in BMDMs from WT and AβPP/PS1 mice. IL-4 significantly increased expression of Arg1 (A) and MRC1 (B) mRNA and MRC1 (C) on BMDMs from WT and AβPP/PS1 mice ($^{***}p < 0.001$; ANOVA; $n = 10$–12), however no genotype-related differences in response to IL-4 were observed. No significant difference in IL-4Rα mRNA expression was observed in BMDMs prepared from AβPP/PS1, compared with WT, mice. Values are means ± SEM.

Genotype-related increases in BBB permeability and chemokines may induce infiltration of macrophages into the brain

Importantly, the data indicate that there was a significant increase in the number of $CD11b^{+}$ $CD45^{high}$ macrophages in brain tissue prepared from AβPP/PS1, compared with WT, mice. While there is no definitive marker which unequivocally distinguishes macrophages from microglia, it is agreed that the relative expression of CD45 is a useful indicator, since it is expressed at much lower levels in resident microglia [36]. Recent data from this laboratory have confirmed a genotype-related increase in the infiltration of macrophages, T lymphocytes, and natural killer cells in AβPP/PS1 mice [22, 33, 34, 37]. Although the mechanism underpinning cell infiltration remains to be clarified, we demonstrate that it is associated with a genotype-related increase in BBB permeability as assessed by extravasation of gadolinium. In other studies from this laboratory [15, 17, 28], increased microglial activation has been accompanied by an increase in IL-12 concentration which may trigger macrophages to release IFNγ [38]. The evidence indicates that microglia in these animals have characteristics of the M1 activation state [39]. A compromised BBB is associated with infiltrating cells [16, 26, 39–41] and the creation of a chemotactic gradient across the BBB further facilitates cell infiltration. Here, increased expression of IP-10 and MCP-1, which are chemotactic for macrophages, is described in tissue from AβPP/PS1 mice and these changes contribute to the development of such a gradient. Additionally, serum from AβPP/PS1 mice, in which inflammatory cytokine concentrations were elevated, was shown to negatively impact on TJ protein expression in a mouse endothelial cell line. These data raise the possibility that circulating factors in the blood of AβPP/PS1 mice may contribute to the loss of integrity of the BBB. During pathological conditions, cytokines can dysregulate the barrier-forming cells resulting in reorganization of junctions, matrix, focal adhesion or release of barrier-modulating factors including matrix metalloproteases [42]. Previous evidence from this laboratory has demonstrated increased BBB disruption in the hippocampus, which is associated with peripheral

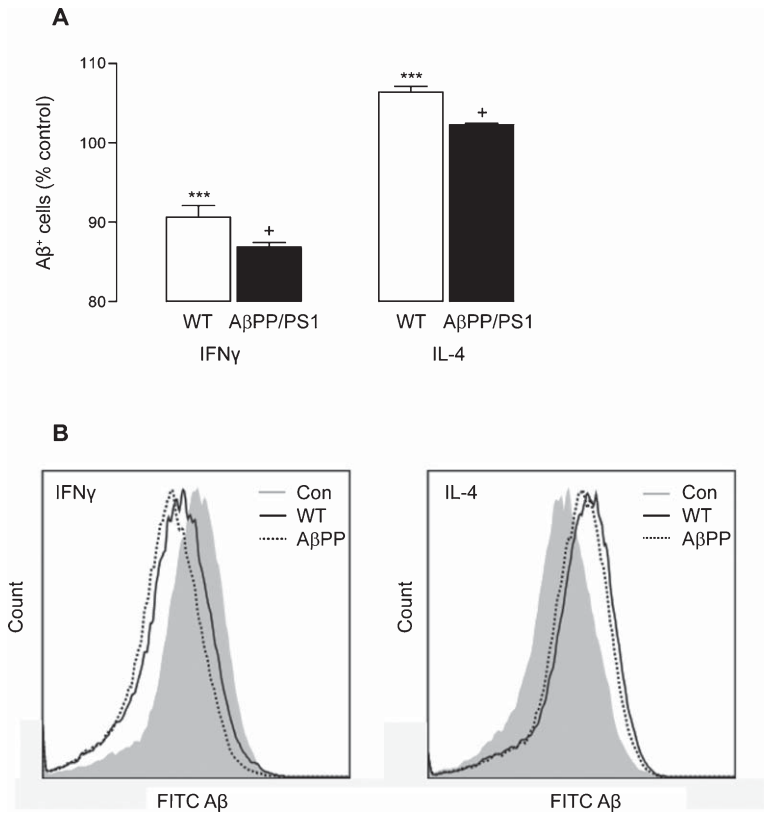

Fig. 6. Phagocytosis of FITC-labelled Aβ is decreased in IFNγ- and enhanced in IL-4-stimulated BMDMs. BMDMs were stimulated with IFNγ (50 ng/ml; 24 h) or IL-4 (200 ng/ml; 24 h) and incubated with FITC-labelled Aβ (2 h). Phagocytosis of FITC-Aβ by BMDMs was significantly decreased by IFNγ and increased by IL-4, compared with vehicle-treated BMDMs ($^{***}p < 0.001$; ANOVA; $n = 4$). The decrease in phagocytosis of FITC-labelled Aβ induced by IFNγ was more profound, while the increase induced by IL-4 was less apparent, in cells prepared from AβPP/PS1 mice ($^{+}p < 0.05$; ANOVA; $n = 4$). Representative histograms are shown in (B).

cell infiltration, neuroinflammatory changes [43], and genotype-associated increases in the same chemokines identified in this study. It is worth noting that BBB permeability was increased in several areas of the brain of AβPP/PS1 mice, though this was not observed in the thalamus (Kelly et al., personal communication).

BMDMs from AβPP/PS1 mice are hypersensitive to M1, but not M2, polarizing stimuli

A significant finding is that the response of BMDMs prepared from AβPP/PS1 mice to IFNγ, an M1 polarizing stimulus, was greater than in cells from WT mice, with evidence of a genotype-related increase in several archetypal markers of this state including TNFα, NOS2, NOD2, and CD86 mRNA [29]. While IFNγ induced release of TNFα and IL-1β from BMDMs prepared from AβPP/PS1 mice, this was not the case in cells from WT mice. While these data suggest that BMDMs from AβPP/PS1 mice are more responsive to IFNγ, it must be acknowledged that the concentration of IFNγ (50 ng/ml) is much greater than that found in the brain (although lower concentrations of IFNγ have a similar effect). An additional limitation is that the effect of IFNγ alone is assessed even though genotype-related increased concentrations of several inflammatory cytokines, which could act synergistically with IFNγ, have been reported [34]. Interestingly, we have found that IL-1β and TNFα act synergistically with IFNγ in macrophages prepared from rats (Costello et al., personal communication). The modest IFNγ-induced release of TNFα described here is consistent with previous findings which demonstrate that IFNγ does not trigger significant release of TNFα [44], but acts as a priming stimulus, inducing its transcription so as to allow a rapid response to a subsequent stimulus. We suggest that the production of inflammatory cytokines by macrophages that infiltrate the brain of AβPP/PS1 mice will add to the pre-existing inflammatory milieu and additionally may play a role

in presenting antigen to T cells, thus further contributing to the developing neuroinflammation.

M2 activation is triggered by the anti-inflammatory cytokines IL-4, IL-5, and IL-13 and characterized by upregulation of markers such as Arg1 and MRC1 [5]. Predictably, IL-4 increased expression of both markers in BMDMs although there was no difference in its effect on cells from WT and AβPP/PS1 mice, underscoring the specificity of the genotype-related response to IFNγ. IL-4Rα mRNA expression was found to be comparable in BMDMs from AβPP/PS1 and WT mice and this may explain why these cells respond to IL-4 stimulation in a similar manner. While the authors are unaware of any previous work investigating the responses of macrophages from AβPP/PS1 mice to inflammatory stimuli, recent evidence from this laboratory has shown that macrophages in the AβPP/PS1 brain exhibit increased expression of CD80 and CD68, both of which are considered markers of activation [33]. The current data using BMDMs replicates published work on microglia from this laboratory [22], which demonstrated that microglia from AβPP/PS1 mice exhibit an enhanced response to IFNγ, as evidenced by increased phosphorylation of signal transducers and activators of transcription (STAT)1. Furthermore, it was also found that the response of microglia from WT and AβPP/PS1 mice to IL-4 was unchanged, reinforcing the present data.

The inflammatory microenvironment in the brain may induce macrophages to adopt the M1 phenotype and contribute to inflammation in AβPP/PS1 mice

These findings have identified that, even after several days in culture, BMDMs prepared from AβPP/PS1 mice exhibit increased expression of IFNγR1 mRNA and that these cells respond more profoundly to IFNγ in a manner that suggests a genotype-related bias toward adopting an M1 phenotype. The importance of this lies in the fact that macrophages infiltrate the brain of AβPP/PS1 mice and encounter an inflammatory environment that has the ability to drive the cells toward the M1 activation state. It is interesting to speculate that the cells are primed by the increase in circulating cytokines and/or Aβ which has been described in these mice (Table 1) and others [45]. In the context of traumatic injury to the spinal cord, it has been suggested that the inflammatory environment suppresses the M2 phenotype [11], with the predominant M1 phenotype limiting repair. Recent data from our laboratory have demonstrated that macrophages which gain entry to the brain of AβPP/PS1 mice exhibit enhanced expression of activation markers [33], while there is no change in the expression of the M2 phenotypic marker, MRC1 [22]. Previous studies have suggested that infiltrating macrophages have an important role in the clearance of Aβ plaques [6, 7], however our data indicate that IFNγ-treated BMDMs are less capable of phagocytosing FITC-labelled Aβ than those treated with IL-4. This is consistent with earlier observations which report that macrophages stimulated with LPS and IFNγ exhibit decreased ability to phagocytose Aβ, whereas those stimulated with IL-4 and IL-13 are more effective phagocytes [46] and that macrophages prepared from AD patients exhibit a decreased ability to clear Aβ [47]. Interestingly, transplanted cells from bone marrow have been shown to contribute to microglial stimulation in AβPP/PS1 mice [48]. It seems likely, based on our observations, that macrophages from AβPP/PS1 mice may adopt an inflammatory phenotype when they infiltrate the brain and consequently, may no longer be effective in clearing the brain of neurotoxic Aβ peptide.

ACKNOWLEDGMENTS

This work was funded by Science Foundation Ireland (07/IN.1/B949). JPB was the recipient of a Trinity College Postgraduate student award. CR was supported by Coordenação de Aperfeiçoamento de Pessoal de Nível Superior (CAPES) and Universidade Federal da Bahia (UFBA), Brazil.

Authors' disclosures available online (http://www.j-alz.com/disclosures/view.php?id=2583).

REFERENCES

[1] Varin A, Gordon S (2009) Alternative activation of macrophages: Immune function and cellular biology. *Immunobiology* **214**, 630-641.

[2] Gordon S, Martinez FO (2010) Alternative activation of macrophages: Mechanism and functions. *Immunity* **32**, 593-604.

[3] Lynch MA (2009) The multifaceted profile of activated microglia. *Mol Neurobiol* **40**, 139-156.

[4] Colton CA, Wilcock DM (2010) Assessing activation states in microglia. *CNS Neurol Disord Drug Targets* **9**, 174-191.

[5] Chhor V, Le Charpentier T, Lebon S, Ore MV, Celador IL, Josserand J, Degos V, Jacotot E, Hagberg H, Savman K, Mallard C, Gressens P, Fleiss B (2013) Characterization of phenotype markers and neuronotoxic potential of polarised primary microglia *in vitro*. *Brain Behav Immun* **32**, 70-85.

[6] Simard AR, Soulet D, Gowing G, Julien JP, Rivest S (2006) Bone marrow-derived microglia play a critical role in restricting senile plaque formation in Alzheimer's disease. *Neuron* **49**, 489-502.

[7] El Khoury J, Toft M, Hickman SE, Means TK, Terada K, Geula C, Luster AD (2007) Ccr2 deficiency impairs microglial accumulation and accelerates progression of Alzheimer-like disease. *Nat Med* **13**, 432-438.

[8] Yong VW, Rivest S (2009) Taking advantage of the systemic immune system to cure brain diseases. *Neuron* **64**, 55-60.

[9] Schwartz M, Kipnis J, Rivest S, Prat A (2013) How do immune cells support and shape the brain in health, disease, and aging? *J Neurosci* **33**, 17587-17596.

[10] Shechter R, London A, Varol C, Raposo C, Cusimano M, Yovel G, Rolls A, Mack M, Pluchino S, Martino G, Jung S, Schwartz M (2009) Infiltrating blood-derived macrophages are vital cells playing an anti-inflammatory role in recovery from spinal cord injury in mice. *PLoS Med* **6**, e1000113.

[11] Kigerl KA, Gensel JC, Ankeny DP, Alexander JK, Donnelly DJ, Popovich PG (2009) Identification of two distinct macrophage subsets with divergent effects causing either neurotoxicity or regeneration in the injured mouse spinal cord. *J Neurosci* **29**, 13435-13444.

[12] Garcia-Alloza M, Robbins EM, Zhang-Nunes SX, Purcell SM, Betensky RA, Raju S, Prada C, Greenberg SM, Bacskai BJ, Frosch MP (2006) Characterization of amyloid deposition in the APPswe/PS1dE9 mouse model of Alzheimer disease. *Neurobiol Dis* **24**, 516-524.

[13] Jankowsky JL, Melnikova T, Fadale DJ, Xu GM, Slunt HH, Gonzales V, Younkin LH, Younkin SG, Borchelt DR, Savonenko AV (2005) Environmental enrichment mitigates cognitive deficits in a mouse model of Alzheimer's disease. *J Neurosci* **25**, 5217-5224.

[14] Cao D, Lu H, Lewis TL, Li L (2007) Intake of sucrose-sweetened water induces insulin resistance and exacerbates memory deficits and amyloidosis in a transgenic mouse model of Alzheimer disease. *J Biol Chem* **282**, 36275-36282.

[15] Gallagher JJ, Minogue AM, Lynch MA (2013) Impaired performance of female APP/PS1 mice in the Morris water maze is coupled with increased Abeta accumulation and microglial activation. *Neurodegener Dis* **11**, 33-41.

[16] Blau CW, Cowley TR, O'Sullivan J, Grehan B, Browne TC, Kelly L, Birch A, Murphy N, Kelly AM, Kerskens CM, Lynch MA (2012) The age-related deficit in LTP is associated with changes in perfusion and blood-brain barrier permeability. *Neurobiol Aging* **33**, 1005 e1023-1035.

[17] Kelly RJ, Minogue AM, Lyons A, Jones RS, Browne TC, Costello DA, Denieffe S, O'Sullivan C, Connor TJ, Lynch MA (2013) Glial activation in AbetaPP/PS1 mice is associated with infiltration of IFNgamma-producing cells. *J Alzheimers Dis* **37**, 63-75.

[18] Lyons A, Murphy KJ, Clarke R, Lynch MA (2011) Atorvastatin prevents age-related and amyloid-beta-induced microglial activation by blocking interferon-gamma release from natural killer cells in the brain. *J Neuroinflammation* **8**, 27.

[19] Cowley TR, O'Sullivan J, Blau C, Deighan BF, Jones R, Kerskens C, Richardson JC, Virley D, Upton N, Lynch MA (2012) Rosiglitazone attenuates the age-related changes in astrocytosis and the deficit in LTP. *Neurobiol Aging* **33**, 162-175.

[20] Brown KL, Poon GF, Birkenhead D, Pena OM, Falsafi R, Dahlgren C, Karlsson A, Bylund J, Hancock RE, Johnson P (2011) Host defense peptide LL-37 selectively reduces proinflammatory macrophage responses. *J Immunol* **186**, 5497-5505.

[21] Lyons A, Griffin RJ, Costelloe CE, Clarke RM, Lynch MA (2007) IL-4 attenuates the neuroinflammation induced by amyloid-beta *in vivo* and *in vitro*. *J Neurochem* **101**, 771-781.

[22] Minogue AM, Jones RS, Kelly RJ, McDonald CL, Connor TJ, Lynch MA (2014) Age-associated dysregulation of microglial activation is coupled with enhanced blood-brain barrier permeability and pathology in APP/PS1 mice. *Neurobiol Aging* **35**, 1442-1452.

[23] Henry CJ, Huang Y, Wynne A, Hanke M, Himler J, Bailey MT, Sheridan JF, Godbout JP (2008) Minocycline attenuates lipopolysaccharide (LPS)-induced neuroinflammation, sickness behavior, and anhedonia. *J Neuroinflammation* **5**, 15.

[24] McMahon EJ, Suzuki K, Matsushima GK (2002) Peripheral macrophage recruitment in cuprizone-induced CNS demyelination despite an intact blood-brain barrier. *J Neuroimmunol* **130**, 32-45.

[25] Gabrusiewicz K, Ellert-Miklaszewska A, Lipko M, Sielska M, Frankowska M, Kaminska B (2011) Characteristics of the alternative phenotype of microglia/macrophages and its modulation in experimental gliomas. *PLoS One* **6**, e23902.

[26] Murphy AC, Lalor SJ, Lynch MA, Mills KH (2010) Infiltration of Th1 and Th17 cells and activation of microglia in the CNS during the course of experimental autoimmune encephalomyelitis. *Brain Behav Immun* **24**, 641-651.

[27] de Vries HE, Blom-Roosemalen MC, van Oosten M, de Boer AG, van Berkel TJ, Breimer DD, Kuiper J (1996) The influence of cytokines on the integrity of the blood-brain barrier *in vitro*. *J Neuroimmunol* **64**, 37-43.

[28] O'Reilly JA, Lynch M (2012) Rosiglitazone improves spatial memory and decreases insoluble Abeta(1-42) in APP/PS1 mice. *J Neuroimmune Pharmacol* **7**, 140-144.

[29] Chhor V, Le Charpentier T, Lebon S, Ore MV, Celador IL, Josserand J, Degos V, Jacotot E, Hagberg H, Savman K, Mallard C, Gressens P, Fleiss B (2013) Characterization of phenotype markers and neuronotoxic potential of polarised primary microglia *in vitro*. *Brain Behav Immun* **32**, 70-85.

[30] Moreira LO, Zamboni DS (2012) NOD1 and NOD2 signaling in infection and inflammation. *Front Immunol* **3**, 328.

[31] Michaud JP, Bellavance MA, Prefontaine P, Rivest S (2013) Real-time *in vivo* imaging reveals the ability of monocytes to clear vascular amyloid beta. *Cell Rep* **5**, 646-653.

[32] Stalder AK, Ermini F, Bondolfi L, Krenger W, Burbach GJ, Deller T, Coomaraswamy J, Staufenbiel M, Landmann R, Jucker M (2005) Invasion of hematopoietic cells into the brain of amyloid precursor protein transgenic mice. *J Neurosci* **25**, 11125-11132.

[33] McManus RM, Higgins SC, Mills KH, Lynch MA (2014) Respiratory infection promotes T cell infiltration and amyloid-beta deposition in APP/PS1 mice. *Neurobiol Aging* **35**, 109-121.

[34] Minogue AM, Jones RS, Kelly RJ, McDonald CL, Connor TJ, Lynch MA (2014) Age-associated dysregulation of microglial activation is coupled with enhanced blood-brain barrier permeability and pathology in APP/PS1 mice. *Neurobiol Aging* **35**, 1442-1452.

[35] Zhu Y, Obregon D, Hou H, Giunta B, Ehrhart J, Fernandez F, Mori T, Nikolic W, Zhao Y, Morgan D, Town T, Tan J (2011) Mutant presenilin-1 deregulated peripheral immunity exacerbates Alzheimer-like pathology. *J Cell Mol Med* **15**, 327-338.

[36] Sedgwick JD, Schwender S, Imrich H, Dorries R, Butcher GW, ter Meulen V (1991) Isolation and direct characterization of resident microglial cells from the normal and inflamed central nervous system. *Proc Natl Acad Sci U S A* **88**, 7438-7442.

[37] Browne TC, McQuillan K, McManus RM, O'Reilly JA, Mills KH, Lynch MA (2013) IFN-gamma Production by amyloid beta-specific Th1 cells promotes microglial activation and

increases plaque burden in a mouse model of Alzheimer's disease. *J Immunol* **190**, 2241-2251.

[38] Darwich L, Coma G, Pena R, Bellido R, Blanco EJ, Este JA, Borras FE, Clotet B, Ruiz L, Rosell A, Andreo F, Parkhouse RM, Bofill M (2009) Secretion of interferon-gamma by human macrophages demonstrated at the single-cell level after costimulation with interleukin (IL)-12 plus IL-18. *Immunology* **126**, 386-393.

[39] Denieffe S, Kelly RJ, McDonald C, Lyons A, Lynch MA (2013) Classical activation of microglia in CD200-deficient mice is a consequence of blood brain barrier permeability and infiltration of peripheral cells. *Brain Behav Immun* **34**, 86-97.

[40] Kroenke MA, Carlson TJ, Andjelkovic AV, Segal BM (2008) IL-12- and IL-23-modulated T cells induce distinct types of EAE based on histology, CNS chemokine profile, and response to cytokine inhibition. *J Exp Med* **205**, 1535-1541.

[41] Togo T, Akiyama H, Iseki E, Kondo H, Ikeda K, Kato M, Oda T, Tsuchiya K, Kosaka K (2002) Occurrence of T cells in the brain of Alzheimer's disease and other neurological diseases. *J Neuroimmunol* **124**, 83-92.

[42] Chaitanya GV, Cromer W, Wells S, Jennings M, Mathis JM, Minagar A, Alexander JS (2012) Metabolic modulation of cytokine-induced brain endothelial adhesion molecule expression. *Microcirculation* **19**, 155-165.

[43] Berner MD, Sura ME, Alves BN, Hunter KW Jr (2005) IFN-gamma primes macrophages for enhanced TNF-alpha expression in response to stimulatory and non-stimulatory amounts of microparticulate beta-glucan. *Immunol Lett* **98**, 115-122.

[44] Berner MD, Sura ME, Alves BN, Hunter KW Jr (2005) IFN-gamma primes macrophages for enhanced TNF-alpha expression in response to stimulatory and non-stimulatory amounts of microparticulate beta-glucan. *Immunol Lett* **98**, 115-122.

[45] Trinchese F, Liu S, Battaglia F, Walter S, Mathews PM, Arancio O (2004) Progressive age-related development of Alzheimer-like pathology in APP/PS1 mice. *Ann Neurol* **55**, 801-814.

[46] Durafourt BA, Moore CS, Zammit DA, Johnson TA, Zaguia F, Guiot MC, Bar-Or A, Antel JP (2012) Comparison of polarization properties of human adult microglia and blood-derived macrophages. *Glia* **60**, 717-727.

[47] Fiala M, Lin J, Ringman J, Kermani-Arab V, Tsao G, Patel A, Lossinsky AS, Graves MC, Gustavson A, Sayre J, Sofroni E, Suarez T, Chiappelli F, Bernard G. (2005) Ineffective phagocytosis of amyloid-beta by macrophages of Alzheimer's disease patients. *J Alzheimers Dis* **7**, 221-232; discussion 255-262.

[48] Malm TM, Koistinaho M, Parepalo M, Vatanen T, Ooka A, Karlsson S, Koistinaho J (2005) Bone-marrow-derived cells contribute to the recruitment of microglial cells in response to beta-amyloid deposition in APP/PS1 double transgenic Alzheimer mice. *Neurobiol Dis* **18**, 134-142.